Image Analysis of Unusual Structures on the Far Side of the Moon near the Crater Paracelsus C

Mark J. Carlotto[1], Francis L. Ridge[2] and, Ananda L. Sirisena[3]
The Lunascan Project and Society For Planetary SETI Research

ABSTRACT

The authors present an analysis of Apollo 15 and Lunar Reconnaissance Orbiter images of two unusual features near the crater Paracelsus C on the far side of the moon. At first glance these structures appear to be walls or towers on the lunar surface. By combining multiple images we show the larger feature, oriented in a northeast/southwest direction, is not simply a wall but two walls on either side of a narrow valley or "passageway". Using single image shape from shading and 3D terrain visualization we show in a computer generated perspective view looking northeast that the southwest end appears to be the entrance to the passageway. A reverse angle view looking southwest shows the passageway ending at a rise of terrain at the other end, possibly leading underground. The terrain surrounding the two structures is not flat but appears "excavated" by some unknown means, natural or artificial. By means of a statistical background model it is shown that these objects are visually different from the lunar background because their underlying structure is different.

1. Introduction

The search for extra-terrestrial intelligence (SETI) began in the 1960s with radio-telescopes (Drake 1960) and has, to date, produced no positive evidence of its existence. During these early years of SETI, Sagan (1963) spoke about the possibility of extraterrestrial visitation

"It is not out of the question that artifacts of these visits still exist, or even that some kind of base is maintained (possibly automatically) within the solar system to provide continuity for successive expeditions. Because of weathering and the possibility of detection and interference by the inhabitants of the Earth, it would be preferable not to erect such a base on the Earth's surface. The Moon seems one reasonable alternative. Forthcoming high resolution photographic reconnaissance of the Moon from space vehicles – particularly of the back side – might bear these possibilities in mind."

---

[1] mark@carlotto.us
[2] skyking42@gmx.com
[3] anandals@aol.com

Foster (1972) estimated frequencies of visitations by extraterrestrials or their messenger probes and suggested the possibility that past encounters may have left behind artifacts or indirect evidence (e.g., deranged planetary terrain). Seeking a broader alternative to radio SETI, a search for extraterrestrial artifacts (SETA) was proposed in the 1980s (Freitas 1983). The search for alien artifacts on the moon (Arkhipov 1998, Davies and Wagner, 2013) is an outgrowth of this more inclusive search strategy.

Davies (2012) has called for a citizen science approach to SETI stating "rather than leaving SETI to a small and heroic band of radio astronomers, we should mobilize the entire scientific community to 'keep their eyes open' for telltale signs of alien technological activity." One suggestion is to look for evidence of mining or quarrying activities. Where on Earth the evidence may be buried beneath overlaying strata, Davies believes "Quarrying or construction on the moon or asteroids would persist conspicuously for much longer, and scrutiny of the Lunar Reconnaissance Orbiter data would be a useful exercise."

This paper provides evidence supporting the hypothesis that features in the crater Paracelsus C on the far side of the moon may be artificial in origin. Section 2 summarizes the discovery of these features – a case study in citizen science. Many times objects that appear unusual in older lower resolution photographs turn out to be unremarkable in higher resolution digital images. Analysis of LRO images in Section 3 including coregistered and "fused" images at different sun angles reveals this is not the case. The question of artificiality in the context of the surrounding terrain is considered in Section 4. Section 5 presents 3-D visualizations of the features and the surrounding area to assist in their interpretation. Areas for future work are discussed in Section 6.

2. Background

Reports of artificial structures on the moon in Apollo and Lunar Orbiter photographs are not uncommon in the popular press and the Internet. Among the first were George Leonard's 1976 book *Somebody Else is On the Moon* and Fred Steckling's 1981 book *We Discovered Alien Bases on the Moon* that identified a large number of unusual features in Lunar Orbiter and Apollo photographs. Literally hundreds of reports can be found online today, many of which can be traced back to these books.

Independent scientific groups such as The Lunascan Project[4] and Society of Planetary SETI Research[5] investigate reported anomalies on the moon, Mars, and elsewhere. In May 2016, SPSR member Ananda Sirisena notified Lunascan project coordinator Francis Ridge that he had found an article posted on the Internet in 2014 reporting the discovery of unusual features on the surface of the moon near the crater Paracelsus resembling dark "walls" or "towers" photographed by the Apollo 15 astronauts[6].

Digging deeper, Ridge found the actual Apollo 15 panoramic camera image frame number, A15-P-8868, referenced in the article, and determined the coordinates of the features. Sirisena then

---

[4] http://www.astrosurf.com/lunascan/

[5] http://spsr.utsi.edu

[6] http://www.ufosightingsdaily.com/2014/01/new-moon-discovery-of-two-tall.html

identified another Apollo 15 image (AS15-P-8873) over the area taken at a different viewing angle. Two images from different viewing angles proved the features were not an optical illusion. Many times objects that appear unusual in older lower resolution photographs turn out to be unremarkable in higher resolution digital images. This was clearly not the case when Ridge found a more recent and much higher resolution Lunar Reconnaissance Orbiter (LRO) image. The features appeared even more unusual up close. Three additional LRO M-frames were found using the Planetary Imagery Processing Environment (PIPE). In total, four LRO M-frames, two Apollo 15 P-frames, and five Apollo metric camera M-frames were located over the area (Table 1).

3. Preliminary Image Analysis

Fig. 2a and Fig. 2b are two map-projected images of the features of interest M118769870L and M1168450258L, respectively. North is up. The larger feature (A) is oriented in a northeast/southwest direction. The smaller features (B) to the south is oriented in a northwest/southeast direction. In M118769870L and M1115441699L the sun is to the west-northwest, illuminating the northwest side of feature A. In M1153132512R and M1168450258L the sun is east-northeast, illuminating the southeast side of A. At this sun angle the terrain to the north casts a shadow along the northwest side.

Using LRO image M1153132512R and associated metadata, the length of A is:

$$L = M \times R = 235 \text{ pixels} \times 0.55 \text{ meters/pixel} \ = \ 129 \text{ meter} \qquad (1)$$

where M is its measured length in pixels and R is the pixel resolution. The length of B is 77 meters.

The height of A can be calculated from the measured length of its shadow, N. Assuming for the moment the shadow is cast on flat terrain, the height at the northeast end is

$$H = \frac{N \times R}{\tan \phi_i} = \frac{132 \text{ pixels} \times 0.55 \text{ meters/pixel}}{\tan 68.9°} = 28.65 \text{ meters} \qquad (2)$$

where ϕ_i is the solar incidence angle. The height at the southwest end is about 19 meters. The height of the southwest end of A estimated from M1168450258L is 31.1 meters, which within a 10% error. Interestingly the height of B is slightly higher, about 29.5 meters.

Registering and combining multiple images reveal new information about these structures that is not evident in the original images. In Fig. 2c the two images have been merged by replacing shadowed pixels in one image with non-shadowed pixels in the other image, and vice versa. In Fig. 2a the sun is to the left, in Fig. 2b the sun is to the right. The resultant merged image reveals A is not simply a "wall" but appears to be two "walls" on either side of a narrow valley or "passageway" (Fig. 3a). B appears to have a ridge-like depression in the middle similar to A as shown in Fig. 3b. These details are discussed further in Section 5.

4. Lunar Context

These features are in the southwest corner of a 24 km crater named Paracelsus C. Paracelsus C is one of number of "satellite" craters of Paracelsus, an impact crater on the far side of the moon (Fig. 4). It is located in the Aitken basin – one of the largest, oldest and deepest basin on the Moon (Petro and Pieters, 2004). With reference to Fig. 5 the area is geologically diverse, containing rolling terrain with a moderately high density of craters less than 20 km in diameter (Nt), smooth light plains (Ip), and uplifted and complex faulted pre-basin bedrock covered by basin ejecta (NpNbr). Given the complexity of the terrain, is it possible that these features are simply uplifted bedrock surrounded by smooth plains?

Although it is not possible to definitely determine the origin of these features from the imagery it can be shown that they are quantitatively different from the surrounding terrain. Sagan (1975) argued that deviations from thermodynamic equilibrium are a necessary (but not sufficient) condition of intelligent activity. He cited significant deviations from the blackbody radiation curve of Earth in the radio frequency portion of the electromagnetic spectrum as evidence of terrestrial intelligence, and went on to show that passive (electro-optical) imaging of Earth at resolutions (spatial scales) smaller than about 1 km reveals evidence of mechanical disequilibrium (e.g., rectilinear patterns of agriculture, road networks, etc.).

Stein (1987) developed an algorithm that models images as fractals. Images of natural backgrounds, like the backgrounds themselves, exhibit a property known as self-similarity that have a distinctive power spectral density

$$S(f) \propto f^{5-2D} \tag{3}$$

where $2 < D < 3$. Deviations from this curve, like that from blackbody radiation indicate possible non-natural, i.e., artificial phenomena. Stein's algorithm has been used in several SETA investigations (Carlotto and Stein, 1990) and (Arkhipov, 1998).

Analysis of the statistics of natural terrestrial backgrounds (forested areas, drainage patterns, tectonic features, etc.) and artificial features (e.g., roads, cities, vehicles, archaeological ruins) reveal artificial structures produce anisotropies in the 2D power spectrum at particular scales or resolutions (Carlotto 2007). A biologically-inspired target screener (Carlotto 2010) models the background using a bank of 64 Gabor filters, which measure the local power spectral density (4 scales x 16 directions). The detection statistic

$$d = (\mathbf{x} - \mathbf{m})^T \mathbf{C}^{-1} (\mathbf{x} - \mathbf{m}) \tag{4}$$

measures the deviation from the background, which is modeled as a Gaussian random variable with mean **m** and covariance **C**. The algorithm detects areas in the image containing objects with non-isotropic power spectra like buildings and vehicles (Fig. 6). Fig. 7 is the result of applying the same algorithm to a portion of LRO frame M118769870L. The area is 4096x4096 pixels at 0.55 meters/pixel or about 507 sq. km. The local power spectra of the features under study as well as several nearby craters appear to deviate significantly from that of the lunar background. These objects are visually different from the background because their underlying structure is different.

5. Three-Dimensional Analysis

Viewing the data in 3D further aids in our ability to understand the shape of these structures and their relation to the background. Two images at different sensor angles and similar sun angles can be viewed side by side in stereo[7]. The Apollo 15 images AS15-P-8868 and AS15-P-8873 are good candidates for stereo as they were acquired from opposite (but unknown) viewing angles ("fore" and "aft") at the same sun angle. Although feature A is only about 10 pixels in size in the P frames and even smaller in the lower resolution M frames it is apparent that the features are not towers but linear structures slightly lower in elevation than the terrain to the east (Fig. 8).

Available elevation maps of the moon do not have sufficient detail to resolve the features under study. Shape from shading (SFS), also called photoclinometry, is another method of extracting height information from images (Horn 1977). SFS is useful in situations where the reflectance characteristics and albedo are uniform across the scene and the image is acquired at or near nadir. SFS methods assume an underlying scene reflectance function relating gradient space to image space. Pentland (1988) derives a linear approximation for the Lambertian reflectance function, which is a good model for matte surfaces. A similar linear approximation can be derived for the lunar surface. Embedding this within a strip integration algorithm described by Horn (1977) we computed height maps from the two merged LRO images, M118769870L and M1168450258L and averaged them together to create a relative height surface. (It is noted that another method known as photometric stereo (Horn 1979) can be used to compute height maps from multiple images acquired at the same (overhead) viewing angle and different solar angles. The set of four LRO images over this area would be good candidates for photometric stereo.)

At this point synthetic views can be generated in any viewing direction by an oblique parallel projection of the merged image mapped onto the height surface (Foley and Van Dam 1983). Fig. 9a is a view at a 40° elevation angle looking northeast. From this viewing angle the southwest end of feature A appears to be the entrance to the passageway. Fig. 9b is a reverse angle view looking southwest that seems to show the passageway ending at the rise of terrain at the other end, possibly leading underground.

Full pixel resolution northeast views of the two structures are shown in Fig. 10. There is insufficient information in the imagery to determine the depth of the valley in between the two walls. It is also not possible to determine if the valley ends or leads underground. The 3D view of feature B reveals a radically different shape from that of A. What appears to be a long thin depression is in fact a steep cliff. The top of B is concave with a rim along the opposite side. The terrain surrounding the two structures is not flat but appears "excavated" by some unknown mechanism.

Fig. 11 is a perspective view of a wider area containing the features of interest. The terrain is not unlike that around the Bingham Canyon copper mine southwest of Salt Lake City, Utah (Fig. 12). However the area surrounding features A and B do not look at all like a terrestrial mine with its terraced sides. That this area is an extinct alien mining or mineral processing operation seems unlikely as similar terracing should be visible in the LRO images on account of the lack of

---

[7] https://en.wikipedia.org/wiki/Stereoscopy

erosional processes on the moon; deposition can be ruled out as the features themselves are clearly visible.

6. Discussion

Enormous quantities of lunar and planetary imagery are available to the public by way of the Internet. While enabling a "citizen science" approach to SETI, the availability of so much data also tends to generate new "discoveries" on a regular basis by those who want to discover something such as alien bases, towers, construction and other activities on the lunar surface. Although most turn out to be camera aberrations, JPEG compression errors, image enhancement artifacts, or simply misinterpretations of unfamiliar surface features imaged in unfamiliar ways, some remain unexplained.

A decidedly conservative mainstream scientific establishment often rejects anomalies based on subject matter alone, i.e., there cannot be ET artifacts on the moon because there are no ET artifacts on the moon (or other planets). Such a view is an example of circular reasoning, based on an assumption that ET does not exist, or if it does exist could not have traveled to our solar system or even evolved within our solar system.

In order to carry out an objective search for artificial features on the moon and planetary surfaces, objective detection criteria must be established. Such criteria have been proposed for radio SETI (Sagan 1975). However, SETI in itself has been criticized on epistemological grounds, i.e., we are looking for what we think is out there (Denton 1984). Since we do not really know what we are looking for, it is not possible to define in a direct way what is artificial. The development and application of anomaly detection algorithms based on fractal (Stein 1987), statistical (Carlotto 2007), and biologically-inspired models (Carlotto 2010) provide necessary but not sufficient evidence of artificiality. However they could be used by a global citizen science community to develop a list of candidate sites for more in-depth investigation. We believe this area in Paracelsus C is one such candidate worthy of future study by orbital missions and surface rovers.

References

Carl Sagan, "Direct contact among galactic civilizations by relativistic interstellar spaceflight," *Planetary and Space Science*, Vol. 11, pp 485-498, 1963.

G. V. Foster, "Non-human artifacts in the solar system," *Spaceflight*, Vol. 14, pp 447-453, Dec. 1972.

C. Sagan, "The recognition of extraterrestrial intelligence", *Proceedings of the Royal Society*, 189, pp.143-153, 1975.

B. K. P. Horn, "Understanding image intensities," *Artificial Intelligence*, Vol. 8, pp 201-231, 1977.

B. K. P. Horn, "Hill shading and the reflectance map," *Image Understanding Workshop*, Palo Alto, CA 1979.

6. R. A. Freitas, "If they are here, where are they? Observational and search considerations," *Icarus*, Vol. 55, pp 337-343, 1983.

J. D. Foley and A. Van Dam, *Fundamentals of Interactive Computer Graphics*, Addison-Wesley, Reading, MA, 1983.

T. Denton, "Dancing in our lenses: Why there are not more technological civilizations," *Journal of the British Interplanetary Society*, Vol. 37, pp 522-525, 1984.

M. C. Stein, "Fractal image models and object detection," *Society of Photo-optical Instrumentation Engineers*, Vol. 845, pp 293-300, 1987.

A. Pentland, "The transform method for shape-from-shading," *MIT Media Lab Vision Sciences Tech. Report 106*, July 15, 1988.

Mark J. Carlotto and Michael C. Stein, "A method for searching for artificial objects on planetary surfaces," *Journal of the British Interplanetary Society*, Vol. 43, pp 209-216, 1990.

A. V. Arkhipov, Earth-moon system as a collector of alien artefacts, *Journal of the British Interplanetary Society*, Vol. 51, pp 181–184, 1998.

Noah E. Petro and Carle M. Pieters, "Surviving the heavy bombardment: Ancient material at the surface of South Pole – Aitken Basin," *Journal of Geophysical Research*, Vol. 109, 2004.

Mark J. Carlotto, "Detecting Patterns of a Technological Intelligence in Remotely-Sensed Imagery," *Journal of the British Interplanetary Society*, Vol. 60, pp 28-39, 2007.

Mark Carlotto, , "BiTS - A Biologically-Inspired Target Screener for Detecting Manmade Objects in Natural Clutter Backgrounds," *SPIE Defense and Security*, 5-9 April 2010, Orlando, Florida (Paper 7697-37).

P.C.W. Davies, "Footprints of alien technology," *Acta Astronautica*, Vol. 73, pp 250–257, 2012.

P. C. W Davies and R. V. Wagner, "Searching for alien artifacts on the moon," *Acta Astronautica*, Vol. 89, pp 261-265., 2013

Table 1 Apollo and LRO images over the area of interest

Frame	Resolution (meters)	Solar Elevation[8]	Emission Angle[9]	Incidence Angle[10]	Phase Angle[11]
AS15-P-8868		14	(forward)		
AS15-P-8873		14	(aft)		
AS15-M-0081	6.4	14			
AS15-M-0082	6.3	14			
AS15-M-0083	6.3	15			
AS15-M-0084	6.5	16			
AS15-M-0085	6.5	16			
M118769870L	0.55		1.7	68.9	70.5
M1115441699L	0.8		1.7	34.4	35.8
M1153132512R	0.94		1.2	58.7	57.6
M1168450258L	0.90		1.7	54.6	56.3

---

[8] Angle between ray directed toward the sun and the surface of the moon.
[9] Look angle of ray directed toward the sensor and the local surface normal (nadir).
[10] 90° – solar elevation angle.
[11] Angle between the emission and incidence angle.

Fig. 1 LRO image search using Planetary Imagery Processing Environment (PIPE)

| a) M118769870L | b) M1168450258L | c) Combined |
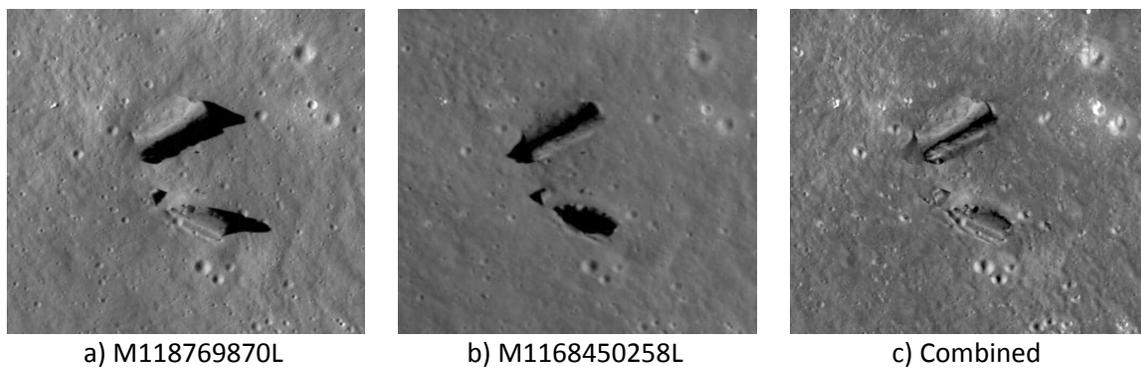
Fig. 2 Merging registered map projected images using shadow pixel replacement (north is up)

| a) Feature A | b) Feature B |
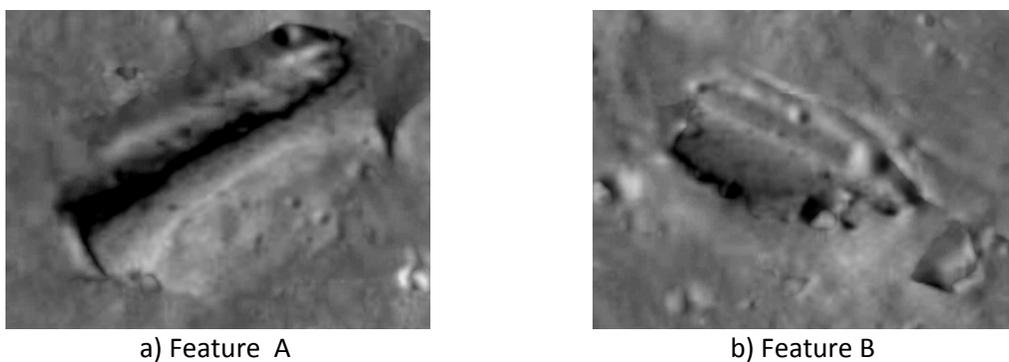
Fig. 3 Close up (full pixel resolution) combined images of the two features. Images have been rotated to the viewing direction (north is down).
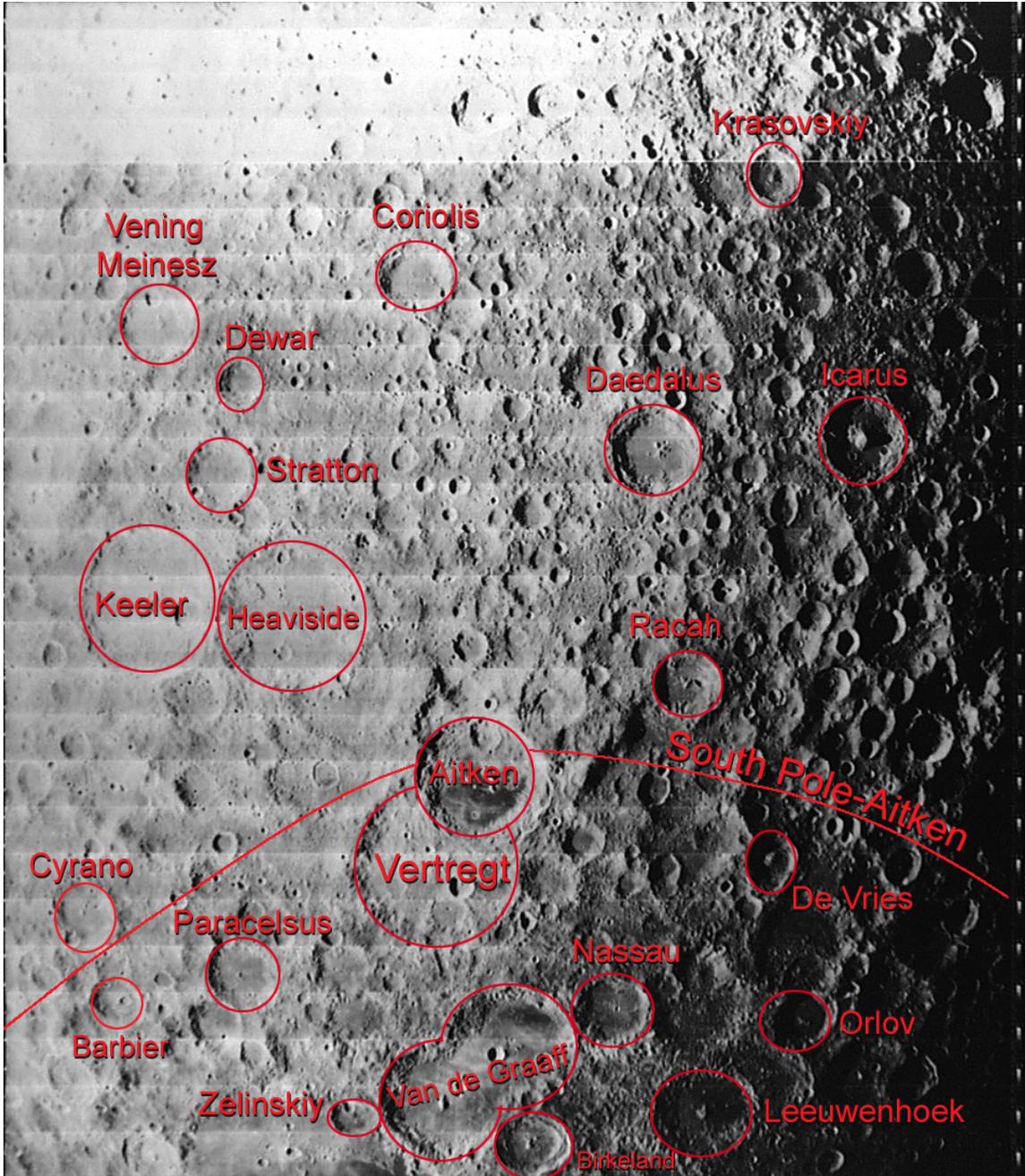
Fig. 4 Paracelsus C is a satellite crater of Paracelsus located in the Aitken basin on the far side of the Moon.
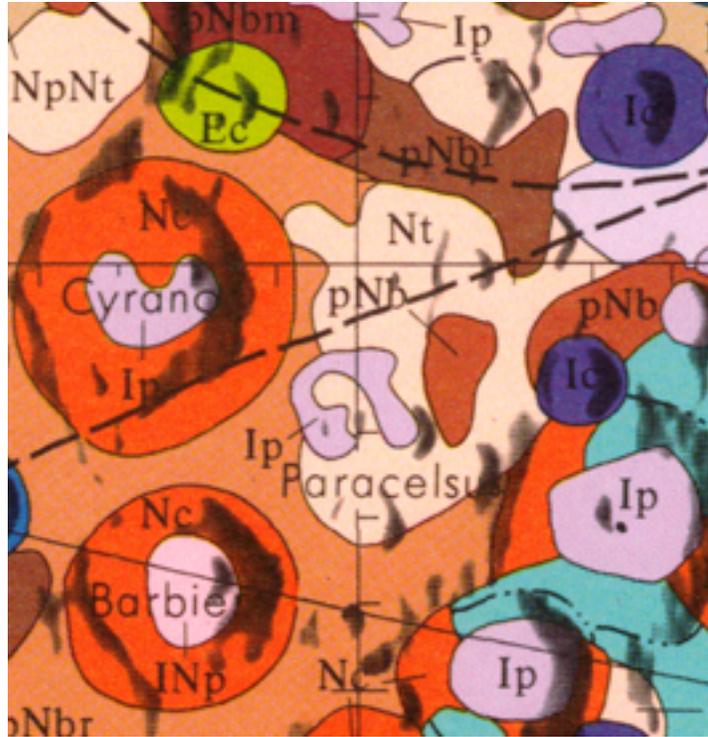
Fig. 5 Section of Geologic Map of the Central Far Side of the Moon[12] over the crater Paracelsus.
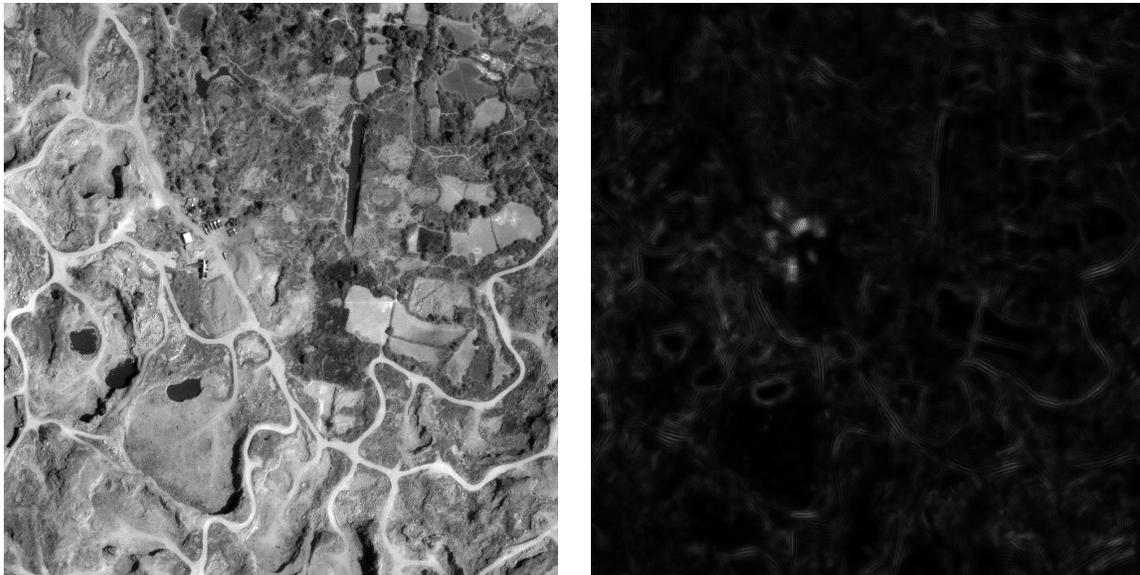
Fig. 6 Small buildings and vehicles in GeoEye image (left). Deviations from background model (right).

---

[12] http://www.lpi.usra.edu/resources/mapcatalog/usgs/
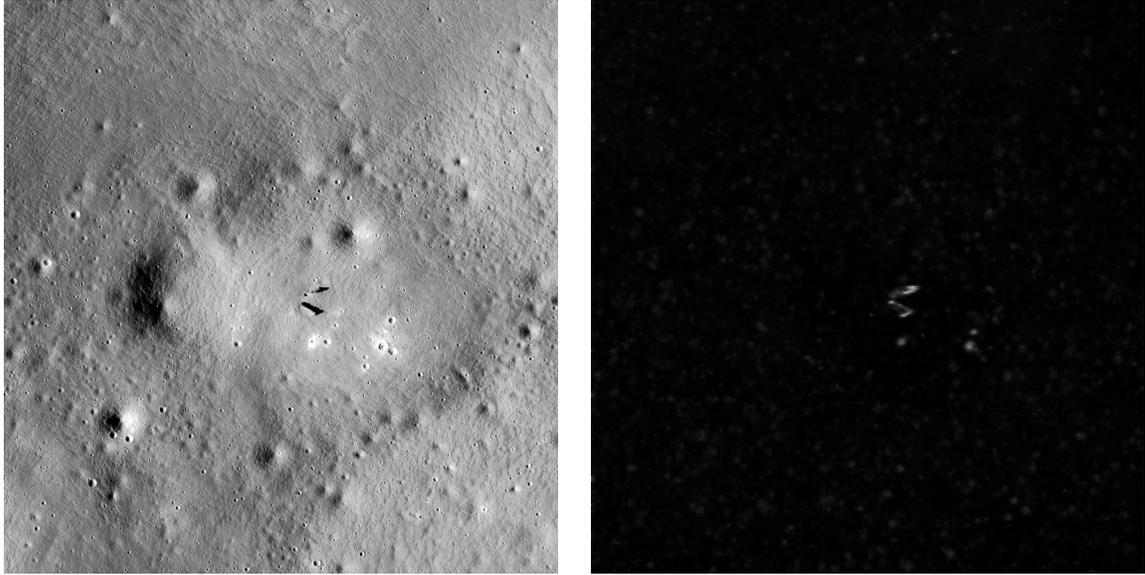
**Fig. 7 Portion of LRO image M118769870L centered over structures (left). Deviations from background model (right).**
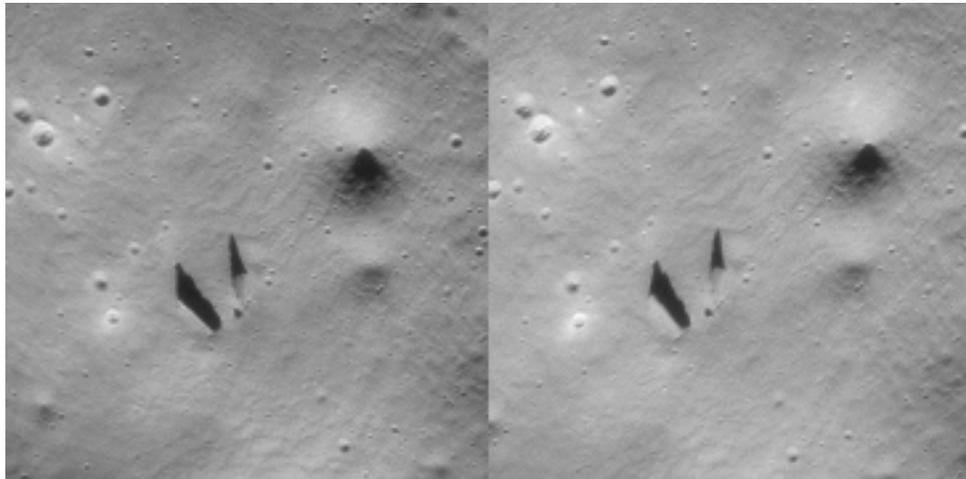
**Fig. 8 Stereo pair constructed from AS15-P-8868 and AS15-P-8873. View is looking west.**

a) 40° elevation angle view looking northeast
b) 50° elevation angle view looking southwest
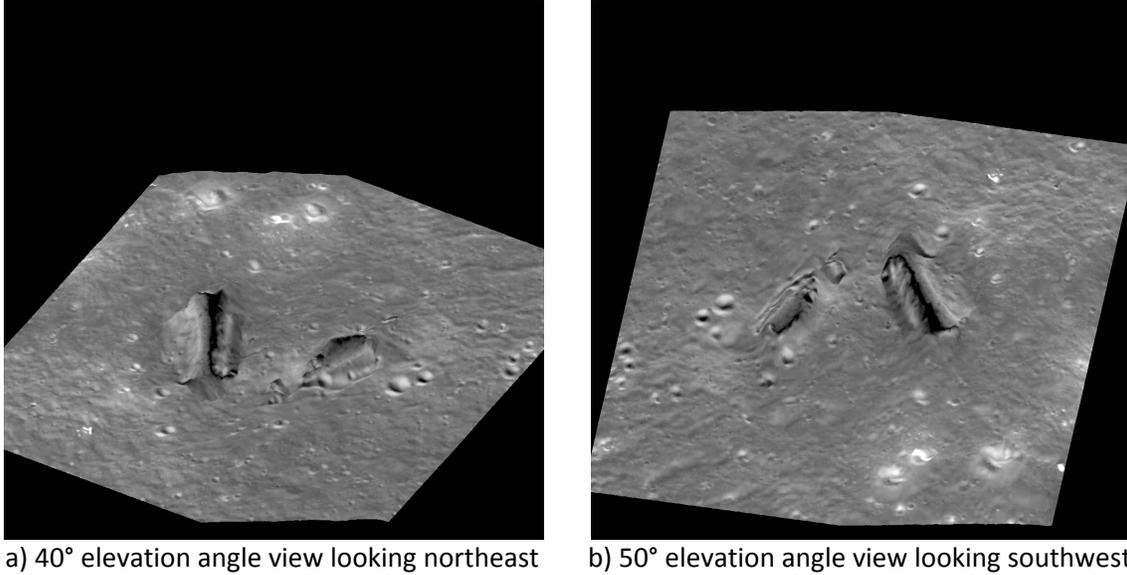
Fig. 9 Two synthesized oblique views computed from the merged image and SFS-derived height map


a) Feature A
b) Feature B
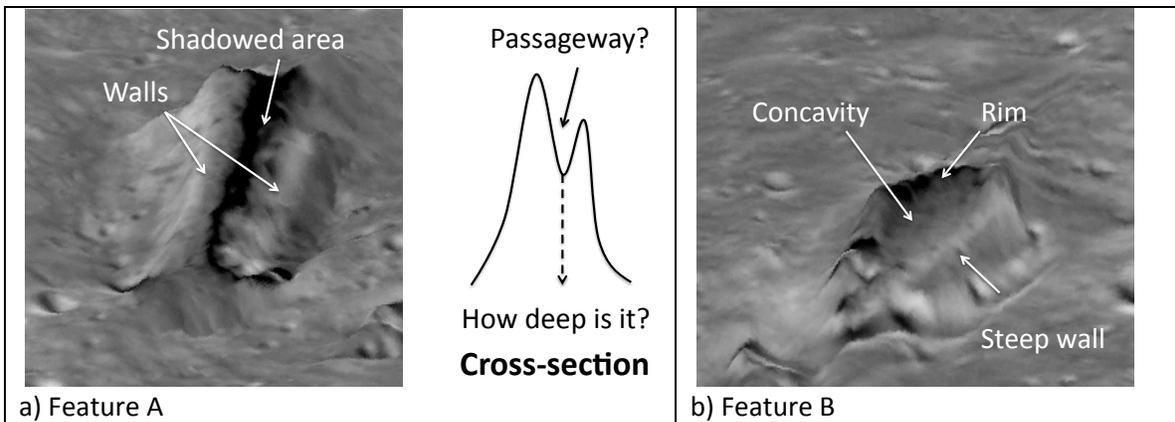
Fig. 10 Details of 3D renderings in 40° elevation angle northeast view
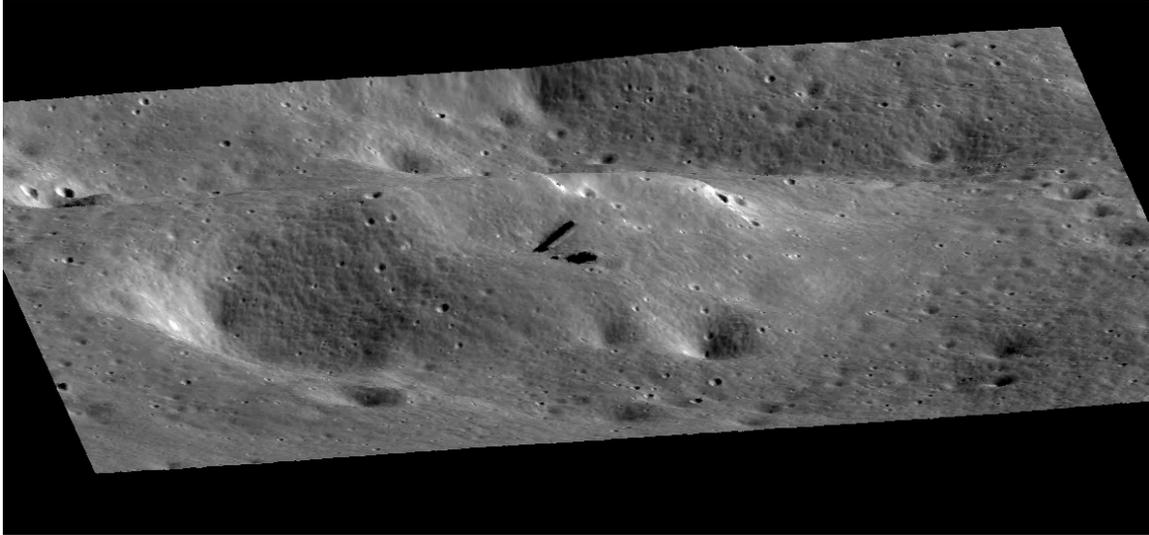
Fig. 11 Perspective view of surrounding area generated from M118769870L . Features A and B are in the middle.

Fig. 12 Bingham Canyon Mine, Utah, USA (Image courtesy Michael Lynch)[13]

---

[13] http://whenonearth.net/awe-inspiring-aerial-images-worlds-mega-mines/